

# **Role of Anterior Chamber Angle Assessment Techniques in Diagnosis of Angle - Closure Glaucoma**

**Essay**

**Submitted by**

**Moataz Hamed Mohamed**  
**(M.B., B.CH.)**

**In Partial Fulfillment of Master Degree in Ophthalmology**

**Under Supervision of**

**Prof. Dr. Mostafa Mostafa Bahgat**

Professor of Ophthalmology  
Faculty of Medicine  
Cairo University

**Assistant Prof. Dr. Amr Abd EL- latif Osman**

Assistant Professor of Ophthalmology  
Faculty of Medicine  
Cairo University

**Dr. Amanne Feisal Esmael**

Lecturer of Ophthalmology  
Faculty of Medicine  
Cairo University

**Cairo University**  
**Faculty of Medicine**  
**2010**

# **Abstract**

Angle-closure glaucoma is a leading cause of irreversible blindness. Diagnosis and treatment are strongly related to angle assessment techniques

## **Gonioscopy:**

Gonioscopy is the current reference standard for assessing ACA structures and configuration. It requires a subjective assessment by an observer placing a contact lens on the eye of the patient. Definitions of angle findings vary across grading schemes. Gonioscopy is prone to potential measurement errors including artificially opening the angle or closing the angle due to how the lens is placed on the eye. (Friedman & Mingguang , 2008)

## **Key Words:**

**Outflow Apparatus Anatomy, Anterior chamber angle assessment techniques, Comparative studies of different techniques of angle assessment**

# Acknowledgement

I would like to express my real and deepest gratitude, respect and appreciation to **Professor Dr. Mostafa Mostafa Bahgat, Professor of Ophthalmology, Cairo University**, for his valuable advices, continuous support, scientific additions and sincere help throughout the work.

My profound thanks and deep gratitude to **Professor Dr. Amr Abd EL- latif Osman, Assistant Professor of Ophthalmology, Cairo University**, for his fruitful assistance and valuable suggestions.

My deepest gratitude to **Dr. Amanne Feisal Esmael Lecturer of Ophthalmology, Cairo University**, for her fruitful advices and support.

Special thanks to all my **Professors, colleagues and staff members in the Ophthalmology Department, Faculty of medicine, Cairo University**, for their encouragement and help.

*Moataz Hamed*

# **Table of contents**

<b>List of abbreviations.</b>	<b>II</b>
<b>List of tables.</b>	<b>IV</b>
<b>List of figures.</b>	<b>V</b>
<b>I. Introduction and Aim of Work.</b>	<b>1</b>
<b>II. Outflow Apparatus Anatomy.</b>	<b>5</b>
<b>III. Anterior chamber angle assessment techniques:</b>	
<b>A. Clinical techniques:</b>	
<b>1. Gonioscopy.</b>	<b>11</b>
<b>2. Limbal Anterior Chamber Depth Measurement (van Herick technique).</b>	<b>23</b>
<b>B. Imaging techniques:</b>	
<b>1. Anterior Chamber Angle Assessment by Ultrasound Biomicroscopy.</b>	<b>25</b>
<b>2. Optical Coherence Tomography Imaging of the Anterior Chamber Angle.</b>	<b>43</b>
<b>3. Scheimpflug Photography of Anterior Chamber Angle.</b>	<b>54</b>
<b>4. Scanning Peripheral Anterior Chamber Depth Analysis.</b>	<b>60</b>
<b>IV. Comparative studies of different techniques of angle assessment.</b>	<b>67</b>
<b>V. Summary.</b>	<b>75</b>
<b>VI. References.</b>	<b>79</b>
<b>Arabic summary.</b>	

## **List of abbreviations**

<b>ACA</b>	anterior chamber angle.
<b>ACD</b>	Anterior chamber depth.
<b>ACG</b>	Angle-closure glaucoma.
<b>ACV</b>	Anterior chamber volume.
<b>AOD</b>	Angle opening distance.
<b>ARA</b>	Angle recess area.
<b>AS-OCT</b>	Anterior segment optical coherence tomography.
<b>ATA</b>	Angle-to-angle distance.
<b>CB</b>	Ciliary body.
<b>CBT</b>	Ciliary body thickness.
<b>CCD</b>	Charge coupled device.
<b>CCT</b>	Central corneal thickness.
<b>CRC</b>	Radius of corneal curvature.
<b>CT</b>	Corneal thickness.
<b>HOCT</b>	High-resolution optical coherence tomography.
<b>IAS</b>	Iridocorneal angle size.
<b>ICPD</b>	Iris–ciliary process distance.
<b>ILA</b>	Iris– lens angle.
<b>ILCD</b>	Iris– lens contact distance.
<b>IOLs</b>	Intraocular lenses.
<b>IZD</b>	Iris–zonule distance.
<b>LACD</b>	Limbal Anterior Chamber Depth Measurement.
<b>LOCT</b>	Low-resolution optical coherence tomography.
<b>LPI</b>	Laser peripheral iridotomy.
<b>PACD</b>	Peripheral anterior chamber deph.
<b>PACG</b>	Primary angle closure glaucoma.
<b>PAS</b>	Peripheral anterior synechia.
<b>PCT</b>	Peripheral corneal thickness.
<b>PIC</b>	Plateau iris configuration.
<b>RPB</b>	Relative pupillary block.
<b>SLD</b>	Superluminescent diode.
<b>SL-OCT</b>	Slitlamp optical coherence tomography.
<b>SPAC</b>	Scanning Peripheral Anterior Chamber Depth Analysis.

<b>TCPD</b>	Trabecular–ciliary process distance.
<b>TIA</b>	Trabecular– iris angle.
<b>TICL</b>	Trabeculo-iris contact length.
<b>TISA</b>	Trabeculo-iris space area.
<b>UBM</b>	Ultrasound biomicroscopy.

## **List of tables**

<b>Table ( 1 )</b>	Advantages and disadvantages of direct and indirect gonioscopy.
<b>Table ( 2 )</b>	Summary of Shaffer system.
<b>Table ( 3 )</b>	Angle grading by van Herick technique.
<b>Table ( 4 )</b>	Parameters proposed by Pavlin et al.

## List of figures

Figure ( 1 )	Stepwise construction of a schematic model, depicting the relationship of structures involved in aqueous humor dynamics.
Figure ( 2 )	Three layers of trabecular meshwork (shown in cutaway views): uveal, corneoscleral, and juxtacanalicular.
Figure ( 3 )	Iris process.
Figure ( 4 )	Diagrammatic representation illustrating the canal of Schlemm.
Figure ( 5 )	A) Koeppe gonioscopes. B) Swan-Jacob gonioscope.
Figure ( 6 )	A) Goldman triple-mirror lens. B) Goldman single mirror lens. C) Zeiss 4-mirror gonioscope.
Figure ( 7 )	Anatomy of the angle structures seen by gonioscopy.
Figure ( 8 )	The corneal wedge.
Figure ( 9 )	Scheie System.
Figure ( 10 )	Shaffer grading of angle width.
Figure ( 11 )	Spaeth system.
Figure ( 12 )	Anterior chamber angle as viewed through the measuring eyepiece for biometric gonioscopy.
Figure ( 13 )	Gonioscopy system using infrared light.
Figure ( 14 )	Modified van Herick scheme.
Figure ( 15 )	UBM appearance of a normal eye.
Figure ( 16 )	Occludable angle with dark room provocative test.
Figure ( 17 )	Pupillary block.
Figure ( 18 )	Plateau iris.
Figure ( 19 )	morphologic changes of iris surface. Before indentation gonioscopy and after indentation gonioscopy; double hump sign.
Figure ( 20 )	Indentation UBM on an eye with a plateau iris.
Figure ( 21 )	Malignant glaucoma.
Figure ( 22 )	Angle closure owing to an iridociliary cyst.
Figure ( 23 )	Ultrasound biomicroscopy images of an eye with relative pupillary block.
Figure ( 24 )	Ultrasound biomicroscopy images of an eye with PAS.
Figure ( 25 )	Pavlin's measurement parameters.
Figure ( 26 )	Schematic illustration and ultrasound biomicroscopy image of the measurement of ciliary body thickness.
Figure ( 27 )	Ultrasound biomicroscopy image of ciliary body of a normal eye and an eye with a narrow angle



Figure ( 28 )	Iris concavity/convexity.
Figure ( 29 )	Limitation of the conventional angle opening distance.
Figure ( 30 )	Angle recess area (ARA).
Figure ( 31 )	Screen shot of the analysis software from the Paradigm UBM.
Figure ( 32 )	Negative acceleration.
Figure ( 33 )	Negative y-intercept.
Figure ( 34 )	The Artemis graphical display.
Figure ( 35 )	Scan profile obtained with the Artemis 2 very high frequency ultrasound system.
Figure ( 36 )	Anterior segment OCT using 1.3 $\mu\text{m}$ wavelength light provides better detail of AC angle anatomy.
Figure ( 37 )	Anterior segment OCT image illustrating AC angle anatomy.
Figure ( 38 )	Angle opening distance at 500 $\mu\text{m}$ and Angle recess area at 500 $\mu\text{m}$ (ARA 500) depicted on OCT image.
Figure ( 39 )	TISA at 500 $\mu\text{m}$ (TISA 500) of a subject with a deep angle recess.
Figure ( 40 )	Trabecular iris contact length depicted on OCT image of a subject with occludable angles on gonioscopy.
Figure ( 41 )	Anterior segment OCT images illustrating a closed AC angle that opens under bright illumination.
Figure ( 42 )	Anterior segment OCT images illustrating a closed AC angle that opens after laser peripheral iridotomy (LPI).
Figure ( 43 )	Detailed angle structures with Fourier-domain OCT.
Figure ( 44 )	The 3D-chamber analysis includes a colored, schematic model of the anterior segment.
Figure ( 45 )	Shallow anterior chamber imaged by pentacam.
Figure ( 46 )	Scheimpflug tomography.
Figure ( 47 )	Pachymetry and correction of the IOP.
Figure ( 48 )	Anterior Chamber Depth map.
Figure ( 49 )	Examples of shallow , normal , and deep anterior chambers evaluated with the Pentacam.
Figure ( 50 )	(A) Configuration of the SPAC system. (B) The photograph of the SPAC equipment.
Figure ( 51 )	Determination of ACD by SPAC.
Figure ( 52 )	Representative SPAC images of a patient with a narrow angle.
Figure ( 53 )	Side-by-side comparison of OCT and UBM images of the AC angle obtained from a single subject.
Figure ( 54 )	Cross-sectional image of the anterior chamber produced by Visante AS-OCT.

Figure ( 55 )	Ultrasound biomicroscopy scan of ACA.
Figure (56 )	Representative images of eyes with narrow angle or wide-open angle. SPAC images are very similar to UBM images.

## **Introduction**

Angle-closure glaucoma (ACG) is a leading cause of irreversible blindness. Diagnosis and treatment are closely related to angle assessment techniques. Different approaches have been developed to aid in the assessment of the anterior chamber angle (ACA). Those approaches include:

1. Clinical techniques:
  - a. Gonioscopy.
  - b. Limbal Anterior Chamber Depth Measurement (LACD), (van Herick Technique).
2. Ultrasound biomicroscopy (UBM).
3. Anterior segment optical coherence tomography (AS-OCT).
4. Pentacam and other devices using Scheimpflug photography.
5. Scanning Peripheral Anterior Chamber Depth Analysis (SPAC)

**Gonioscopy:** is the current reference standard for evaluation of the anterior chamber angle. It has substantial inter-observer variability and relies on subjective assessment of ACA findings.

**Limbal Anterior Chamber Depth Measurement (LACD) (van Herick Technique):** is a quick, easy test that can identify the persons with gonioscopically closed anterior chamber angles and can be used in screening. (Friedman & Mingguang, 2008).

**Ultrasound Biomicroscopy (UBM):** offers tremendous insight into the anterior chamber angle configuration and allows for detailed imaging of the ciliary body and the posterior chamber. Pathophysiologic changes involving anterior segment architecture can be evaluated qualitatively and quantitatively. **(Ishikawa & Schuman, 2004)**

**Anterior Segment Optical Coherence Tomography (AS-OCT):** is an alternative cross-sectional imaging modality that has several advantages over other techniques used for objective assessment of the AC angle. It has a higher image resolution than UBM, is totally noncontact, and is easily performed with minimal expertise. **(Radhakrishnan et al., 2005)**

**Pentacam:** and other device using the rotating Scheimpflug principle can be used in grading of angle width. Although this technique offers a non-contact approach to angle assessment (which is highly appealing for screening purposes), it does not allow detailed visualization of angle structures, compared to UBM. **(Konstantopoulos et al., 2007)**

**Scanning Peripheral Anterior Chamber Depth Analysis (SPAC):** is a new, non-contact, optical alternative method of ACA assessment. The SPAC does not image the angle directly, and therefore does not give detailed information on angle anatomy. **(Friedman and Mingguang, 2008 and Lavanya et al., 2008)**

## **Aim of work**

This is a review of techniques for assessment of the ACA and their role in diagnosis of angle closure glaucoma. Each technique will be discussed along with its currently used parameters. An assessment of the strengths and limitations of each approach will also be provided. Finally, comparisons of findings using the various techniques will be detailed.

## **Outflow Apparatus Anatomy**

### **1- Internal scleral sulcus**

#### **The Sulcus:**

The sulcus is a circular groove on the inner aspect of the corneoscleral limbus, extending from the termination of Descemet's membrane anteriorly (demarcated by Schwalbe's ring) to the scleral spur posteriorly. The sulcus completely accommodates the canal of Schlemm externally, and the corneoscleral portion of the trabecular meshwork internally **Figure ( 1 ).** (Snell and Lemp, 1998)

#### **Schwalbe's ring:**

Schwalbe's ring is the anterior border ring of the trabecular region. The ring marks the transition between the corneal endothelium and the trabecular cells and also the termination of Descemet's membrane. (Shields et al., 2005)

#### **Scleral spur:**

The scleral spur is a wedge-shaped circular ridge which marks the deep aspect of the sclerolimbic junction. It receives the insertion of the anterior tendons of the longitudinal ciliary muscle on its inner aspect. Its anteromedial base forms the posterior margin of the scleral sulcus and receives the posterior attachment of the corneoscleral meshwork. Contraction of the ciliary muscle pulls the spur posteriorly and opens up the trabecular spaces. (Bron et al., 1997)

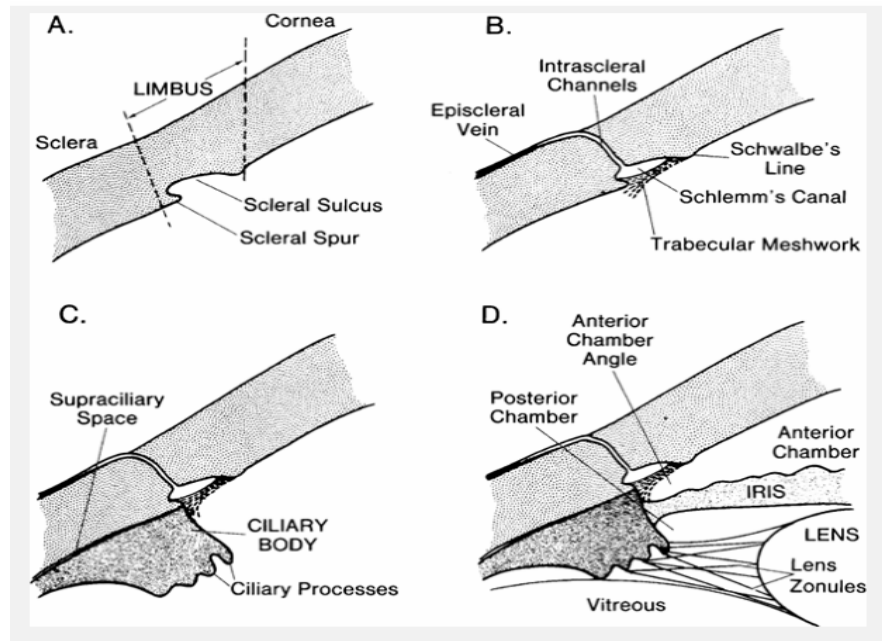


**Figure ( 1 ):** Stepwise construction of a schematic model, depicting the relationship of structures involved in aqueous humor dynamics. A: Limbus. B: Main route of aqueous humor outflow (conventional or trabecular outflow). C: Ciliary body (site of aqueous humor production and other outflow route of the unconventional or uveoscleral outflow). D: Iris and lens. **(Shields et al., 2005)**

## 2- Trabecular meshwork: Figure ( 2 )

The trabecular meshwork is a sponge work of connective tissue beams which are arranged as superimposed perforated sheets. The beams are arranged circularly in the chamber angle and extend from Schwalbe's ring anteriorly to the scleral spur and junction of iris and ciliary body posteriorly. The inner portion of the trabecular meshwork is referred to as the uveal meshwork and the outer portion, connected to the spur and closer to Schlemm's canal, is the corneoscleral meshwork. The spaces of the trabecular meshwork decrease in size progressively from within outwards. **(Bron et al., 1997).**